

Received April 20, 2022, accepted May 9, 2022, date of publication May 13, 2022, date of current version May 18, 2022.

Digital Object Identifier 10.1109/ACCESS.2022.3174861

# Improved Microstrip-to-ESIW Transition With Elliptical Dielectric Taper in Ku- and Ka-Bands

JOSÉ A. BALLESTEROS<sup>1</sup>, ANGEL BELENGUER<sup>1</sup>, (Senior Member, IEEE),  
MARCOS D. FERNANDEZ<sup>1</sup>, HÉCTOR ESTEBAN GONZÁLEZ<sup>2</sup>, (Senior Member, IEEE),  
AND VICENTE E. BORJA<sup>2</sup>, (Fellow, IEEE)

<sup>1</sup>Departamento de Ingeniería Eléctrica, Electrónica, Automática y Comunicaciones, Universidad de Castilla-La Mancha, Escuela Politécnica de Cuenca, Campus Universitario, 16071 Cuenca, Spain

<sup>2</sup>Departamento de Comunicaciones, Universitat Politècnica de València, 46022 València, Spain

Corresponding author: José A. Ballesteros (josea.ballesteros@uclm.es)

This work was supported by the Ministerio de Ciencia e Innovación, Spanish Government, through the Subprojects C44 and C41 of the Coordinated Research and Development Project PID2019-103982RB under Grant MCIN/AEI/10.13039/501100011033.

**ABSTRACT** Empty Substrate Integrated Waveguide (ESIW) technology preserves the many advantages of the Substrate Integrated Waveguide (SIW) such as low cost, low profile, and easy integration with Printed Circuit Boards (PCBs). Moreover, it has additional advantages due to the avoidance of dielectric filling: lower insertion losses and resonators with higher quality factor. In order to connect the ESIW line to classical planar lines, the design of transitions becomes specially important. Due to this, some microstrip-to-ESIW transitions have been published in recent years. Problems of these transitions are usually the complexity of the manufacturing process or increased radiation losses. Knowing the aforementioned disadvantages of the published solutions, in this paper, the transition with an expanded ESIW section has been improved, by adding an easy-to-manufacture dielectric taper that minimizes the undesired radiation losses. Additionally, the new proposed transition can be mechanized easier than previous solutions based on sharp tapers. Moreover, the slight overlap between the microstrip line and the upper ESIW metal cover has been avoided, thus enhancing the return losses of the proposed transition. To validate the proposed transition, two back-to-back prototypes have been manufactured both in Ku- and Ka-band, obtaining insertion losses lower than 0.31 dB and return losses higher than 20.8 dB in Ku-band, and insertion losses lower than 1.36 dB and return losses higher than 14.75 dB in Ka-band.

**INDEX TERMS** Empty substrate integrated waveguide (ESIW), microstrip, transition, elliptical taper, millimeter-waves systems, Ku-band, Ka-band.

## I. INTRODUCTION

Empty Substrate Integrated Waveguide (ESIW) was originally proposed in 2014 [1]. It preserves the main advantages of the Substrate Integrated Waveguide (SIW) [2]: low cost manufacturing, small size and easy integration with other printed circuits in the same substrate. Since the dielectric material has been removed along the propagation path of the guided fields in the ESIW, it exhibits higher performance than an equivalent SIW counterpart, i.e. lower losses and higher quality factor in resonators. Many different devices, such as filters, antennas, directional couplers

or phase-shifters, among others, have been implemented in ESIW technology [3].

Several transitions have been also proposed to connect the ESIW to microstrip lines. The first one consists of a two-stage mode converter, being the microstrip mode transformed into the fundamental mode of the waveguide through a metallic iris followed by an exponential taper, which provides a soft transition between the dielectric of the feeding microstrip line and the empty ESIW. Since this transition fails for thin substrates, another version was proposed in [4] where an additional taper was included in the microstrip feeding line. The third version of this transition was proposed in [5], where two air holes were added to increase its mechanical accuracy, and via holes were used to prevent radiation losses. Another transition based on sharp exponential dielectric taper is the

The associate editor coordinating the review of this manuscript and approving it for publication was Yiming Huo<sup>1</sup>.

multilayer transition [6], in which a transformer in height adapted to the ESIW was included. This transition makes possible the integration of ESIW devices with a higher number of layers, i.e. with increased height and quality factor, but this is not the aim of the transition proposed in this paper.

Apart from these previous versions, directly derived from the original transition, four other transitions have been proposed in the literature. Liu *et al* [7] replaced the sharp dielectric taper by an additional ESIW section of expanded width, which provided a less sensitive solution but at the cost of an increased size and radiation losses. Another transition is proposed in [8], where the ESIW is excited with a through-wire from the microstrip line, which is implemented in an adjacent layer (i.e. in one of the covers of the ESIW). This new transition is compact, less sensitive to manufacturing errors, and more versatile (since any angle between the feeding line and the ESIW can be chosen). Moreover, in the through-wire transition the ESIW and the microstrip feeding line are implemented in different layers. The transition proposed in [9] modifies the solution of [7] using a tapered artificial dielectric slab matrix, reducing the area of the transition, but the cost and complexity of the transition is increased due to the manufacturing process of the rectangular metallic rods in the aluminum plate to create the artificial dielectric slab. The last solution has been recently proposed in [10] with a tapered microstrip transition between the 50 Ω microstrip line and ESIW for impedance and mode matching. The problem of this transition is that the radiation losses are even higher (an 8%) than those for the solution presented in [7].

The disadvantage of the transition with a sharp dielectric taper [5] is related to the difficulty of the manufacturing and soldering processes, which increases the probability of manufacturing errors of the transition. To solve this problem it is possible to think in a blunt transition but, although it solves problems related to the manufacturing process, has a poorer adaptation. Another solution could be an extended transition as the one described by Liu *et al* in [7]. Regarding this transition, a potential drawback is related to the abrupt transition between the microstrip line (filled with dielectric) and the empty waveguide. This discontinuity involves an impedance mismatch, which can cause that part of the incident power is either radiated, or reflected back to the microstrip line, thus reducing the transmitted power to the ESIW.

In this paper, both solutions have been combined by adding an elliptical taper to the transition proposed by Liu *et al* [7]. The elliptical taper mechanically improves previous sharper tapers and the artificial dielectric slab matrix taper, being easier to manufacture with standard printed circuit board (PCB) processes. Moreover, the proposed solution reduces the return and radiation losses, because it improves the impedance matching between the microstrip and the empty integrated waveguide. The only drawback of this transition is the increase in size compared with other transitions apart from the one based in an extended guide. Another advantage of this transition is that the overlap between the taper and the upper cover has been avoided, enhancing the return losses of the

proposed transition, being higher than those of the through-wire transition.

## II. DESIGN OF THE PROPOSED TRANSITION

Figure 1 shows the layout of the central layer of the new transition. As can be observed, it consists of an expanded-width ESIW section and an elliptical dielectric taper. The structure is closed by an upper and a bottom cover manufactured in FR4.

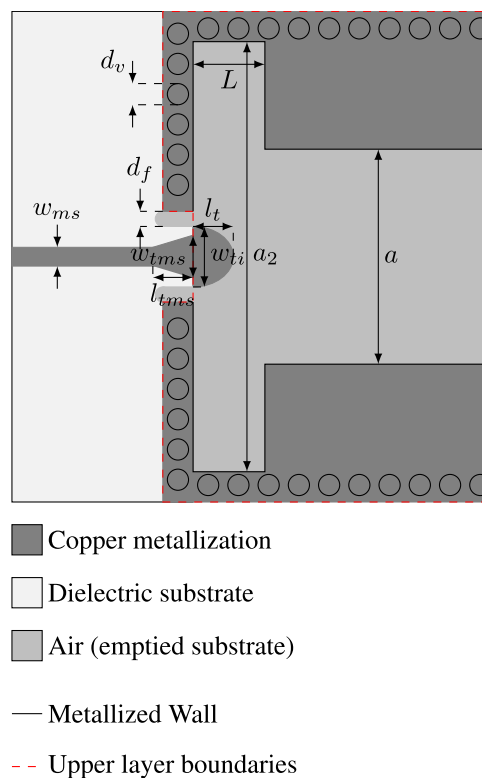


FIGURE 1. Layout of the central layer of the proposed microstrip to ESIW transition.

The design procedure of the proposed transition combines a first taper in the microstrip line with a second tapering structure inside an extended-width ESIW. To do that, the design methods explained in [5] and [7] have been properly adapted. In the proposed transition, the shape of the taper has been modified to be elliptical, which is easier to manufacture. The shape of the taper has been chosen after testing with different shapes, such as sinusoidal ones. Moreover, two holes of diameter  $d_f$  have been mechanized at both sides of the taper, assuring the width of the opening in the back wall of the ESIW. Finally, via holes are designed and manufactured following the same procedure as that for standard SIW vias [11], in order to avoid possible leaky waves traveling through the substrate outside the ESIW.

Apart from all previous contributions, including the elliptical shape of the taper, another improvement of this transition is the fact that there is no overlap between the microstrip line and the upper cover of the ESIW. As it can be seen in Fig. 1, where the upper layer contour is plotted in red, an incision

has been done in the upper layer over the taper, thus avoiding the overlapping with this microstrip part. Nevertheless, outside such area, the overlapping is kept to properly solder both layers, thus increasing the mechanical resistance of the proposed solution. As a result of this non-overlapping, the matching is increased and the transition response, in terms of return losses, is improved.

In order to design the proposed transition, it is important to find a good initial point for the design parameters. Equations (1) to (5) provide good approximations for the design parameters, and can be used to obtain a good initial point. These expressions have been adapted experimentally from those included in [5] and [7].

$$a_2 = 1.5a \tag{1}$$

$$L = \frac{3\lambda_g(f_0)[\text{wider guide}]}{8} \tag{2}$$

$$l_t = l_{tms} = \frac{\lambda_{ms}(f_0)}{4} \tag{3}$$

$$w_{tms} = 0.3a \tag{4}$$

$$w_{ti} = 1.2w_{tms} \tag{5}$$

Expressions (1) to (5) have been used to design two different transitions in a Rogers 4003C substrate. The first one covers the whole frequency range of Ku-band with the same width as the standard WR-62 rectangular waveguide, substrate height of 0.813 mm and copper metallization of 17.5 μm. The second transition is for an ESIW with the width of a WR-28 rectangular waveguide, substrate height of 0.305 mm and copper metallization of 17.5 μm, covering the whole frequency range of Ka-band.

Once initial values are obtained as indicated before, an optimization process is next applied to fine tune the design parameters using the Computer Simulation Technology (CST) Microwave Studio Suite commercial software. In particular, the dimensions that define the transition ( $a_2$ ,  $L$ ,  $l_t$ ,  $l_{tms}$ ,  $w_{ti}$  and  $w_{tms}$ ) have been optimized applying a Nelder Mead Simplex algorithm to maximize return losses and minimize insertion losses. Table 1 shows the values chosen for the fixed geometrical parameters, as well as the initial values obtained with equations (1) to (5), and the final optimum values.

Figure 2 shows the initial and final results obtained for the proposed transitions. These results correspond to simulations made with CST Microwave Studio without losses. It can be observed the good initial points obtained with return losses higher than 15 dB. After the optimization process, both transitions (for WR-28 and for WR-62) provide return losses higher than 30 dB in the whole frequency range of the ESIW.

### III. BACK-TO-BACK PROTOTYPE

To validate the proposed solution, two back-to-back transitions have been designed both in Ku-band (ESIW width  $a = 15.798$  mm) to cover the whole frequency range from 12 to 18 GHz, and in Ka-band (ESIW width  $a = 7.112$  mm) to cover the whole frequency range from 26.5 to 40 GHz. The central layer of the back-to-back transition in

TABLE 1. Dimensions of the two designed transitions.

	Fixed values (dimensions in mm)			
	WR-62		WR-28	
$a$	15.7988		7.1120	
$h$	0.813		0.305	
$w_{ms}$	1.8519		0.6801	
$d_f$	1		0.5	
$d_v$	1		1	
	Optimization parameters (dimensions in mm)			
	WR-62		WR-28	
	Initial	Final	Initial	Final
$a_2$	23.6982	23.3585	10.6680	10.5494
$L$	7.9004	7.9032	3.5649	3.6372
$l_t$	2.9195	3.6529	1.3298	1.7140
$l_{tms}$	2.9195	2.7522	1.3298	1.3032
$w_{ti}$	3.7917	4.1476	1.6323	1.5927
$w_{tms}$	4.7396	5.5883	2.1336	1.9812

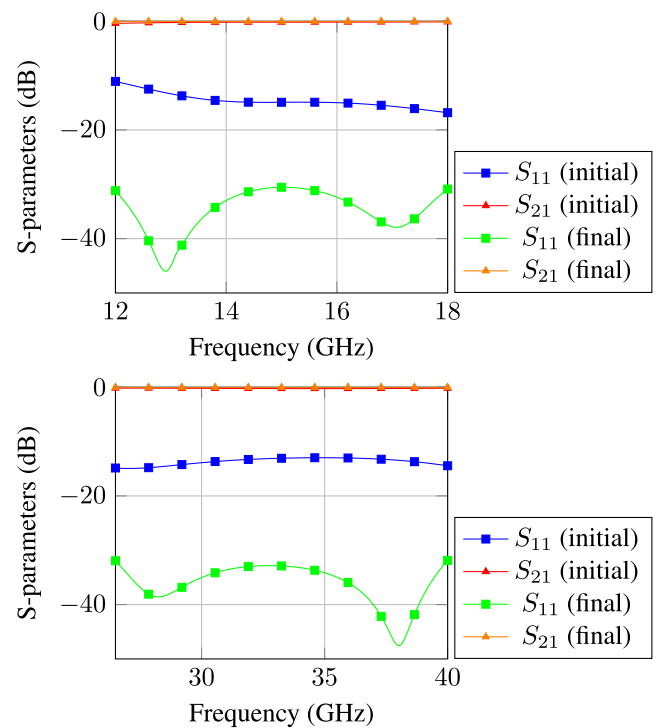


FIGURE 2. Comparison between initial and optimum designs in CST Microwave Studio without losses for WR-62 (top) and for WR-28 (bottom).

Ku-band has been designed using Rogers 4003C substrate, of 0.813 mm height and copper metallization of 17.5 μm; whereas for the Ka-band design a Rogers 4003C substrate, of 0.305 mm height and copper metallization of 17.5 μm, has been used. FR4 substrate, of 1 mm height and copper metallization of 17.5 μm, has been used in both cases for upper and bottom layers. Despite being all layers metallized, additional copper electrodeposition of height 9 μm has been added on each side. Figure 3 shows the manufactured back-to-back transition in Ka-band before assembling, and figure 4 shows the final integrated prototype. The Ku-band prototype has also been manufactured and presents a similar appearance.

Figure 5 shows the comparison between the results for the new proposed transition in Ka-band, compared with those

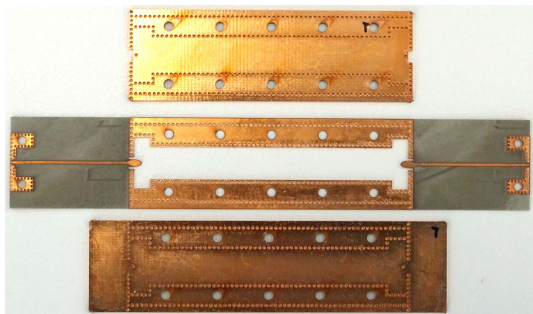


FIGURE 3. Back-to-back prototype in Ka-band of the proposed transition.



FIGURE 4. Assembled back-to-back transition in Ka-band.

of another one based on an elliptical taper without extended guide, and one more based on the solution described in [7] (which has been properly designed to satisfy the Ka-band requirements). The Ka-band has been chosen for performing this comparison because, as the frequency is higher, designs are more sensitive to manufacturing errors. Once a design is validated at higher frequency, it should properly work when the frequency is reduced, as it is less sensitive to the cited manufacturing issues. These results correspond to simulations from CST Microwave Studio without considering losses. The transition with the blunt taper has a poor adaptation with return losses above 12 dB, insertion losses around 0.15 dB, and almost without radiation losses. Although these results are similar to those obtained in [8], the transition with the blunt elliptical taper has not the advantages of the through-wire transition: compactness, freedom to select microstrip and ESIW heights, and possibility of varying the feeding angle. Given that the transition without taper has an abrupt discontinuity between the dielectric and the air transmission media, which implies an impedance mismatch, part of the incident power is lost by radiation increasing the insertion losses. This fact is more important when the frequency is increased, obtaining a power balance lower than 0.92 and insertion losses higher than 0.77 dB at the end of the Ka-band. Combining both solutions, the discontinuity is avoided and the impedance matching is better. The results obtained in this case show a balance higher than 0.995 and insertion losses of 0.056 dB in the worst case, which means that the proposed transition reduces the related insertion losses in 0.71 dB compared with the transition proposed in [7].

Concerning the manufacturing process, since the dielectric taper has an elliptical shape, it is easy to manufacture with standard PCB manufacturing processes, such as drilling, cutting, milling, plating and soldering. The manufacturing complexity is almost the same for both considered transitions (with and without elliptical taper).

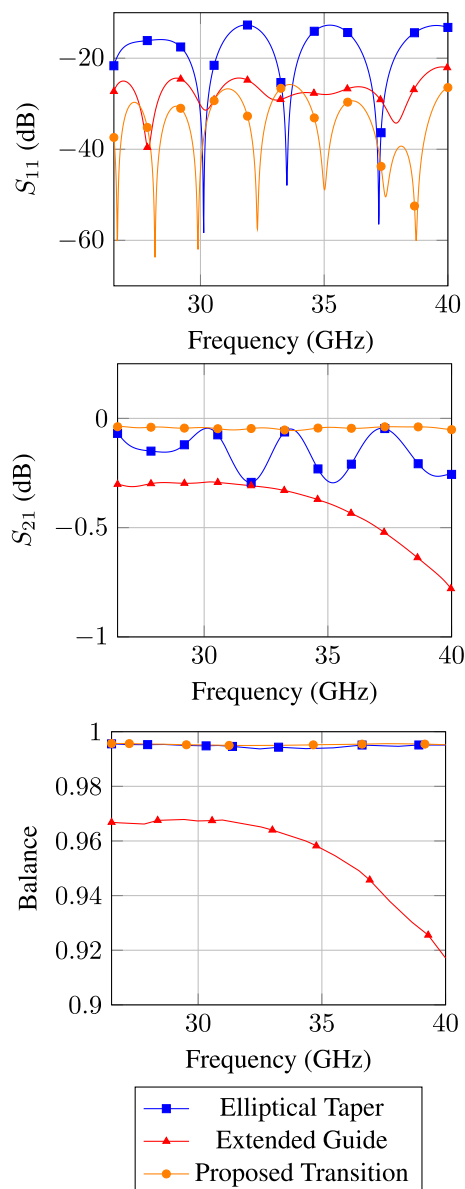


FIGURE 5. Back-to-back comparison (Ka-band) in CST Microwave Studio without losses in terms of  $S_{11}$ ,  $S_{21}$  and balance  $(1 - |S_{11}|^2 - |S_{21}|^2)$ .

To take into account in simulation not only the material losses, but also the effect of the copper roughness [12], each one of the metallic layers of the manufactured filters has been measured with an Accretech Handysurf+ roughness meter. Table 2 shows the mean rms values in microns, where  $Ra$  is the arithmetical mean roughness value,  $Rz$  is the mean roughness depth, and  $Rt$  is the total height of the roughness profile. These results have been included in CST Microwave Studio Suite to take into account the reduced conductivity of the material ( $3.0133 \cdot 10^7$  S/m in Ku-band and  $2.1719 \cdot 10^7$  S/m in Ka-band), instead of the typical value for the conductivity of the copper ( $5.8 \cdot 10^7$  S/m).

Figure 6 shows the measurement results of the two back-to-back prototypes with a network analyzer Anritsu

**TABLE 2. Rugosity measurements (rms values in microns).**

$Ra$	$Rz$	$Rt$
0.3806	2.2942	2.9325

MS4644A using a TRL calibration kit (see figure 7). As it can be observed, there is a good agreement between simulation (considering losses and rugosity) and measurement results. Differences in return losses are due to manufacturing errors that become more important when the frequency range is increased. In the whole Ku-band of the ESIW back-to-back prototype, the measured return losses are greater than 20.8 dB, and insertion losses are smaller than 0.31 dB (i.e. 0.155 dB for each one of the two involved transitions). In Ka-band the measured return losses are greater than 14.75 dB, and insertion losses are smaller than 1.36 dB (i.e. 0.68 dB for each one of the two involved transitions).

A yield analysis was carried out to analyze the robustness of the proposed transition, considering that the dimensions of the elliptical taper and the section of expanded width had a randomized and independent variation given by manufacturing tolerances. It has been assumed that these variations have normal distribution with zero mean and standard deviation of 2 (the laser micromachining process tolerance), 5, 25 and 50 microns. The threshold to consider the quality of the prototypes acceptable is to achieve return losses above 20 dB in the whole frequency band (from 12 GHz to 18 GHz in Ku-band, and from 26.5 GHz to 40 GHz in Ka-band). Table 3 shows the percentage of prototypes that will satisfy the considered quality requirement, being the transition almost insensitive to manufacturing errors in Ku-band. In Ka-band the transition is insensitive to small manufacturing errors (2 and 5 microns), and quite robust when the manufacturing errors are increased (25 and 50 microns), being the tolerances to manufacturing errors lower than in previous transitions (see for example [8]).

**TABLE 3. Results of the yield analysis for the proposed transition (in Ku- and Ka-band).**

Std ( $\mu\text{m}$ )	Ku-band	Ka-band
2	100	100
5	100	100
25	100	90.4
50	97.4	74.3

Table 4 compares our solution with all the previously published microstrip-to-ESIW transitions in terms of number of layers to manufacture the component (complexity), the central frequency of the operational bandwidth, the insertion and return losses of the manufactured back-to-back transition in the whole operational bandwidth of the ESIW, and the total electrical length of the structure (expressed in terms of the free-space wavelength). The table shows the good performance of this transition compared with previous ones. In Ku-band, return losses are similar to the values of other back-to-back prototypes at the same frequency (e.g. [5] and [7]); whereas insertion losses are better than any other

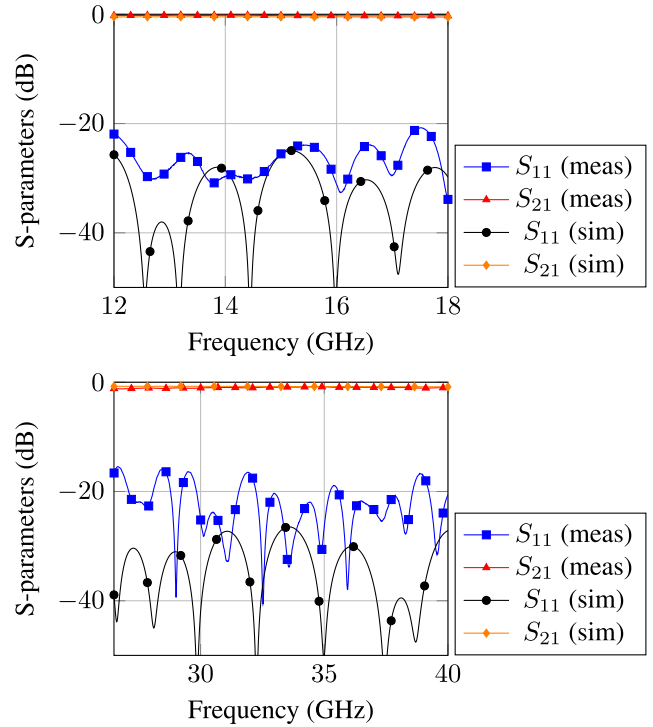


**FIGURE 6. Results of the back-to-back prototypes in Ku-band (top) and Ka-band (bottom).**



**FIGURE 7. TRL calibration kit in Ka-band.**

result. In Ka-band both return and insertion losses are similar to those in [9] operating at the same frequency. Moreover, transition is shorter than those proposed in [7] and [13], of similar length to the solution in [9], and has a higher length than the others. Finally, the manufacturing process is easier than those used in [5], [9] and [13]; and similar to those described in [7], [8] and [10]. All things considered, this transition is the most suitable one to manufacture devices independently of the operating frequency band.

**TABLE 4. Performance comparison of the proposed back-to-back transition with other microstrip-to-ESIW back-to-back transitions.**

Transition	manufacturing complexity	Freq. (GHz)	IL max (dB)	RL (dB)	Length (mm)
[5]	medium	15	1.2	20	0.41·λ <sub>0</sub>
[7]	easy	15	1.08	21	0.66·λ <sub>0</sub>
[8]	easy	10.25	0.9	12	0.32·λ <sub>0</sub>
[9]	difficult	33.25	1.26	14.7	0.55·λ <sub>0</sub>
[10]	easy	10	1.3	15	0.25·λ <sub>0</sub>
[13]	medium	12	1.5	13.5	0.62·λ <sub>0</sub>
<b>(This work Ku)</b>	<b>easy</b>	<b>15</b>	<b>0.31</b>	<b>20.8</b>	<b>0.53·λ<sub>0</sub></b>
<b>(This work Ka)</b>	<b>easy</b>	<b>33.25</b>	<b>1.36</b>	<b>14.75</b>	<b>0.55·λ<sub>0</sub></b>

**IV. CONCLUSION**

In this paper, a new microstrip-to-ESIW transition has been proposed. The combination of an extended-width ESIW with an elliptical taper reduces the radiation losses of the proposed transition, thus enhancing the matching level between the microstrip line and the ESIW. Moreover, the overlap between the upper cover and the taper has been avoided, improving the return loss level in the whole frequency range. In order to validate the proposed solution, both a Ku- and a Ka-band back-to-back transition have been successfully designed and manufactured using standard PCB processes. In the whole Ku-band frequency range (from 12 GHz to 18 GHz), the measured return losses are greater than 20.8 dB, and insertion losses are smaller than 0.31 dB. In Ka-band (from 26.5 GHz to 40 GHz) the measured return losses are greater than 14.75 dB, and insertion losses are smaller than 1.36 dB. Moreover, the yield analysis has shown that the proposed transition is almost insensitive to manufacturing errors in Ku-band, and it is also very robust for Ka-band applications. After the comparison of the proposed transition with others previously published, it can be concluded that this one has better performance independently of the considered frequency range.

**REFERENCES**

[1] A. Belenguer, H. Esteban, and V. E. Boria, "Novel empty substrate integrated waveguide for high-performance microwave integrated circuits," *IEEE Trans. Microw. Theory Techn.*, vol. 62, no. 4, pp. 832–839, Apr. 2014.

[2] D. Deslandes and K. Wu, "Integrated microstrip and rectangular waveguide in planar form," *IEEE Microw. Wireless Compon. Lett.*, vol. 11, no. 2, pp. 68–70, Feb. 2001.

[3] A. Belenguer, H. Esteban, A. Borja, J. Ballesteros, M. Fernandez, J. Morro, J. de Dios, C. Bachiller, and V. Boria, "Empty substrate-integrated waveguides: A low-cost and low-profile alternative for high-performance microwave devices," in *Wiley Encyclopedia of Electrical and Electronics Engineering*. Hoboken, NJ, USA: Wiley, 2020, pp. 1–23, doi: 10.1002/047134608X.W8411.

[4] H. Peng, X. Xia, J. Dong, and T. Yang, "An improved broadband transition between microstrip and empty substrate integrated waveguide," *Microw. Opt. Technol. Lett.*, vol. 58, no. 9, pp. 2227–2231, 2016.

[5] H. Esteban, A. Belenguer, J. R. Sánchez, C. Bachiller, and V. E. Boria, "Improved low reflection transition from microstrip line to empty substrate-integrated waveguide," *IEEE Microw. Wireless Compon. Lett.*, vol. 27, no. 8, pp. 685–687, Aug. 2017.

[6] J. A. Martinez, A. Belenguer, J. J. De Dios, H. E. Gonzalez, and V. E. Boria, "Wideband transition for increased-height empty substrate integrated waveguide," *IEEE Access*, vol. 7, pp. 149406–149413, 2019.

[7] Z. Liu, J. Xu, and W. Wang, "Wideband transition from microstrip line-to-empty substrate-integrated waveguide without sharp dielectric taper," *IEEE Microw. Wireless Compon. Lett.*, vol. 29, no. 1, pp. 20–22, Jan. 2019.

[8] A. Belenguer, J. A. Ballesteros, M. D. Fernandez, H. E. Gonzalez, and V. E. Boria, "Versatile, error-tolerant, and easy to manufacture through-wire Microstrip-to-ESIW transition," *IEEE Trans. Microw. Theory Techn.*, vol. 68, no. 6, pp. 2243–2250, Jun. 2020.

[9] H. Peng, F. Zhao, Y. Liu, S. O. Tatu, and T. Yang, "Robust microstrip to empty substrate-integrated waveguide transition using tapered artificial dielectric slab matrix," *IEEE Microw. Wireless Compon. Lett.*, vol. 30, no. 9, pp. 849–852, Sep. 2020.

[10] A. A. Khan, M. Kahar, and M. K. Mandal, "A modified microstrip to empty substrate integrated waveguide transition," *Int. J. RF Microw. Comput.-Aided Eng.*, vol. 32, no. 2, p. e22990, Feb. 2022, doi: 10.1002/mmce.22990.

[11] F. Xu and K. Wu, "Guided-wave and leakage characteristics of substrate integrated waveguide," *IEEE Trans. Microw. Theory Techn.*, vol. 53, no. 1, pp. 66–73, Jan. 2005.

[12] T. Liang, S. Hall, H. Heck, and G. Brist, "A practical method for modeling PCB transmission lines with conductor surface roughness and wideband dielectric properties," in *IEEE MTT-S Int. Microw. Symp. Dig.*, Jun. 2006, pp. 1780–1783.

[13] H. Peng, X. Xia, S. O. Tatu, K.-D. Xu, J. Dong, and T. Yang, "Broadband phase shifters using comprehensive compensation method," *Microw. Opt. Technol. Lett.*, vol. 59, no. 4, pp. 766–770, Apr. 2017.



**JOSÉ A. BALLESTEROS** received the degree in telecommunications engineering from the Universidad de Alcalá de Henares (UAH), Spain, in 2009, and the Ph.D. degree from the Universidad Politécnica de Madrid (UPM), in 2014. He joined at Universidad de Castilla-La Mancha, in 2007, where he is a Professor Titular de Universidad with the Departamento de Ingeniería Eléctrica, Electrónica, Automática y Comunicaciones. He has authored or coauthored several papers in peer-reviewed international journals and conference proceedings. His research interests include involved with empty substrate integrated waveguide (ESIW) devices and their manufacturing and applications.



**ANGEL BELENGUER** (Senior Member, IEEE) received the degree in telecommunications engineering and the Ph.D. degree from the Universidad Politécnica de Valencia (UPV), Spain, in 2000 and 2009, respectively. He was at Universidad de Castilla-La Mancha, in 2000, where he is a Full Professor with the Departamento de Ingeniería Eléctrica, Electrónica, Automática y Comunicaciones. He has authored or coauthored more than 50 papers in peer-reviewed international journals and conference proceedings and frequently acts as a reviewer for several international technical publications. His research interests include methods in the frequency domain for the full-wave analysis of open-space and guided multiple scattering problems, the application of accelerated solvers or solving strategies (like grouping) to new problems or structures, EM metamaterials, and substrate integrated waveguide (SIW) devices and their applications.



**MARCOS D. FERNANDEZ** received the degree in telecommunications engineering from the Universidad Politécnica de Catalunya (UPC), Spain, in 1996, and the Ph.D. degree from the Universidad Politécnica de Madrid (UPM), in 2006. He was at Universidad de Castilla-La Mancha, in 2000, where he is a Professor Titular de Universidad with the Departamento de Ingeniería Eléctrica, Electrónica, Automática y Comunicaciones. He has authored or coauthored several papers in peer-reviewed international journals and conference proceedings. His research interests include involved with empty substrate integrated waveguide (ESIW) devices and their manufacturing and applications.



**HÉCTOR ESTEBAN GONZÁLEZ** (Senior Member, IEEE) received the degree in telecommunications engineering from the Universidad Politécnica de Valencia (UPV), Spain, in 1996, and the Ph.D. degree in 2002. He worked at the Joint Research Centre, European Commission, Ispra, Italy. In 1997, he was at the European Topic Centre on Soil (European Environment Agency). He rejoined the UPV, in 1998. His research interests include methods for the full-wave analysis

of open-space and guided multiple scattering problems, CAD design of microwave devices, electromagnetic characterization of dielectric and magnetic bodies, the acceleration of electromagnetic analysis methods using the wavelets, and the FMM.



**VICENTE E. BORIA** (Fellow, IEEE) was born in Valencia, Spain, in May 1970. He received the Ingeniero de Telecomunicación (Hons.) and Doctor Ingeniero de Telecomunicación degrees from the Universidad Politécnica de Valencia, Valencia, in 1993 and 1997, respectively. In 1993, he was at the Departamento de Comunicaciones, Universidad Politécnica de Valencia, where he has been a Full Professor, since 2003. In 1995 and 1996, he was holding a Spanish Trainee position at the

European Space Research and Technology Centre, European Space Agency (ESTEC-ESA), Noordwijk, The Netherlands, where he was involved in the area of EM analysis and design of passive waveguide devices. He has authored or coauthored 15 chapters in technical textbooks, 200 articles in refereed international technical journals, and over 250 papers in international conference proceedings. His current research interests include the analysis and automated design of passive components (in particular filters and multiplexers) in several technologies and the simulation and measurement of power effects in high-frequency devices and systems. He has been a member of the IEEE Microwave Theory and Techniques Society (IEEE MTT-S) and the IEEE Antennas and Propagation Society (IEEE AP-S), since 1992. He is also a member of the European Microwave Association (EuMA), and the Chair of the 48th European Microwave Conference held in Madrid, Spain. He acts as a regular reviewer of the most relevant IEEE and IET technical journals on his areas of interest. He was an Associate Editor of IEEE MICROWAVE AND WIRELESS COMPONENTS LETTERS, from 2013 to 2018, and *IET Electronics Letters*, from 2015 to 2018. Currently, he is the Subject Editor (Microwaves) of *IET Electronics Letters*, and the Editorial Board Member of *International Journal of RF and Microwave Computer-Aided Engineering*. He is also a member of the Technical Committees of the IEEE-MTT International Microwave Symposium and of the European Microwave Conference.

• • •